

**DYNAMIC STABILITY OF ROTATING SHAFT UNDER
PARAMETRIC EXCITATION SUBJECTED TO
SPECIFIED BOUNDARY CONDITIONS**

A THESIS SUBMITTED IN PARTIAL FUFILLMENT
OF THE REQUIREMENTS FOR THE DEGREE OF

**Bachelor of Technology
in
Mechanical Engineering**

By
**DINESH KUMAR MANDAL
and
MANIK CHANDRA MAHAPATRA**



**Department of Mechanical Engineering
National Institute of Technology
Rourkela**

2007

**DYNAMIC STABILITY OF ROTATING SHAFT UNDER
PARAMETRIC EXCITATION SUBJECTED TO
SPECIFIED BOUNDARY CONDITIONS**

A THESIS SUBMITTED IN PARTIAL FUFILLMENT
OF THE REQUIREMENTS FOR THE DEGREE OF

**Bachelor of Technology
in
Mechanical Engineering**

By
**DINESH KUMAR MANDAL
and
MANIK CHANDRA MAHAPATRA**

Under the Guidance of
Prof.Sukesh Chandra Mohanty



**Department of Mechanical Engineering
National Institute of Technology
Rourkela**

2007



**National Institute of Technology
Rourkela**

CERTIFICATE

This is to certify that the thesis entitled, “DYNAMIC STABILITY OF ROTATING SHAFT UNDER PARAMETRIC EXCITATION SUBJECTED TO SPECIFIED BOUNDARY CONDITIONS”, submitted by Sri DINESH KUMAR MANDAL and Sri MANIK CHANDRA MAHAPATRA in the partial fulfillment of the requirements for the award of Bachelor of technology Degree in Mechanical Engineering at the National Institute of Technology, Rourkela (Deemed University) is authentic work carried out by them under my supervision and guidance.

To the best of my knowledge the matter embodied in the thesis has not been submitted to any other University/Institute for the award of any Degree or Diploma.

Date:

Prof.S.C.Mohanty
Department of Mechanical Engineering
National Institute of Technology
Rourkela-769008

ACKNOWLEDGEMENT

We avail this opportunity to express our hereby indebtedness, deep gratitude and sincere thanks to **Sri S.C. Mohanty**, Asst. Professor, Department of Mechanical Engineering, National Institute of Technology, Rourkela for his in-depth supervision, constant encouragement, co-operative and pain staking attitude during the entire period of project work and without whom the work would not have been in its present shape.

We are extremely thankful to **Dr. B. K. Nanda**, H.O.D, Dept. of Mechanical Engg. N.I.T, Rourkela and **Dr. K. P. Maity**, Course Co-ordinator for their help and advice during the course of this work

Last but not the least we extend our sincere thanks to all those people who have helped us during all project work and have been involved directly or indirectly in our endeavor.

Manik Chandra Mahapatra
Roll No.-10303017
Dept. of Mechanical Engg.
N.I.T, Rourkela

Dinesh Kumar Mandal
Roll No.-10303032
Dept. of Mechanical Engg.
N.I.T, Rourkela

CONTENTS

CHAPTER	TOPIC	PAGE NO.
	ABSTRACT NOMENCLATURE FIGURE INDEX TABLE INDEX	
CHAPTER 1	INTRODUCTION	1-4
CHAPTER 2 2.1 2.2 2.3	THEORETICAL ANALYSIS FINITE ELEMENT FORMULATION FINITE SHAFT ELEMENT SYSTEMS EQUATION OF MOTION	5-12 5-7 9-10 11-12
CHAPTER 3 3.1 3.2 3.3 3.4	EXPERIMENTAL VALIDATION INTRODUCTION DESCRIPTION OF EXPERIMENTAL SET UP SPECIMEN PREPARATION EXPERIMENTAL PROCEDURE	13-21 13 13 21 21
CHAPTER 4	RESULTS AND DISCUSSION	22-28
CHAPTER 5	CONCLUSION	30
CHAPTER 6	REFERENCES	31-32

ABSTRACT

The dynamic stability behavior of a rotating shaft system under parametric excitation subjected to specified boundary conditions is studied theoretically and theoretical findings with the experimental results. For this theoretical analysis Finite Element Method is applied to derive the governing equation of motion. In this paper, the Ritz finite element procedure and LaGrange's equation are employed to derive the governing equation of a rotating shaft subjected to axial compressive forces. The effects of gyroscopic moment and the static buckling load parameter on the regions of dynamic instability are studied. Application of Bolotin's method and under the conditions of constant rotational speed, the boundaries between the regions of stability and instability are constructed. For experimental work the existing experimental setup is redesigned. Suitable End Attachments are designed and fabricated to achieve various conditions of boundary conditions for the rotating shaft

NOMENCLATURE

E	Modulus of elasticity
I_d	Diametral mass moments of inertial of the shaft per unit length
I_p	Polar mass moments of inertial of the shaft per unit length
L	Length of the shaft
N	Speed of the rotating shaft
P	Axial periodic load
$P(t)$	Axial compressive load
P_o, P_t	Time dependent amplitude of load
P^*, P_{cr}	Fundamental static buckling load
t	Variable time
T^e	Kinetic energy of the shaft
U^e	Potential energy of the shaft
α	Static load factor
β	Dynamic load factor
ρ	Mass density of the material of the beam
Ω	Disturbing frequency
ω_1	Fundamental natural frequency
θ	Axial disturbance frequency

FIGURE INDEX

FIGURE NO.	FIGURE	PAGE NO.
1.1	Graph of Ordinary Resonance	2
1.2	Graph of Parametric Resonance	3
2.1	Schematic Diagram for the Theoretical Analysis	8
3.1	Schematic Diagram for Experimental Setup	14
3.2	Picture for Experimental Setup	15
3.3	AutoCAD diagram for Fixed Motor End	16
3.4	AutoCAD diagram for Fixed Bottom End	17
3.5	AutoCAD diagram for Pinned Motor End	18
3.6	AutoCAD diagram for Pinned Bottom End	19
3.7	Picture of End Attachments	20
4.1	Theoretical Graph for Fixed-Pinned end condition	23
4.2	Theoretical Graph for Fixed-Fixed end condition	24
4.3	Theoretical Graph for Pinned-Pinned end condition	25
4.4	Experimental Graph for Fixed-Pinned end condition	26
4.5	Experimental Graph for Fixed-Fixed end condition	27
4.6	Experimental Graph for Pinned-Pinned end condition	28

TABLE INDEX

TABLE NO.	TABLE	PAGE NO.
4.1	CONFIGURATION DATA, MATERIAL PROPERTIES AND FORMULAE USED	29

Chapter 1

INTRODUCTION

INTRODUCTION

Dynamic stability

The theory of dynamic stability of elastic systems deals with the study of vibrations induced by pulsating loads that are parametric with respect to certain forms of deformation.

Parametric excitation

A system is said to be parametrically excited if the excitation which is a function of time appears as one of the coefficients of the homogenous differential equation describing the system, unlike external excitation which leads to an inhomogeneous equation.

Practical examples

In practice parametric excitation can occur in structural systems subjected to vertical ground motion (drill bit), aircraft structures subjected to turbulent flow, machine components and mechanisms. Other examples are longitudinal excitation of rocket tanks and their liquid propellant by the combustion chambers during powered flight.

Spinning satellites in elliptical orbits passing through a periodically varying gravitational field. In industrial mechanisms, their components and instruments are frequently subjected to periodic excitation transmitted through elastically coupling elements (electromagnetic and aeronautical instruments), vibrator conveyers and saw blades.

Difference between Parametric instability and Typical resonance

In parametric instability the rate of increase is generally exponential and thus potentially dangerous while in typical resonance the rate of increase is linear

Damping reduces the severity of typical resonance but may only reduce the rate of increase during parametric resonance

Parametric instability occurs over a region of parameter space and not at discrete points

Ordinary Resonance

In this case external force is applied transverse to the beam or parallel to the amplitude of vibration which leads to ordinary typical resonance when the excitation frequency becomes equal to the natural frequency of the system. This causes resonance only at discrete point. The figure is shown in the next page.

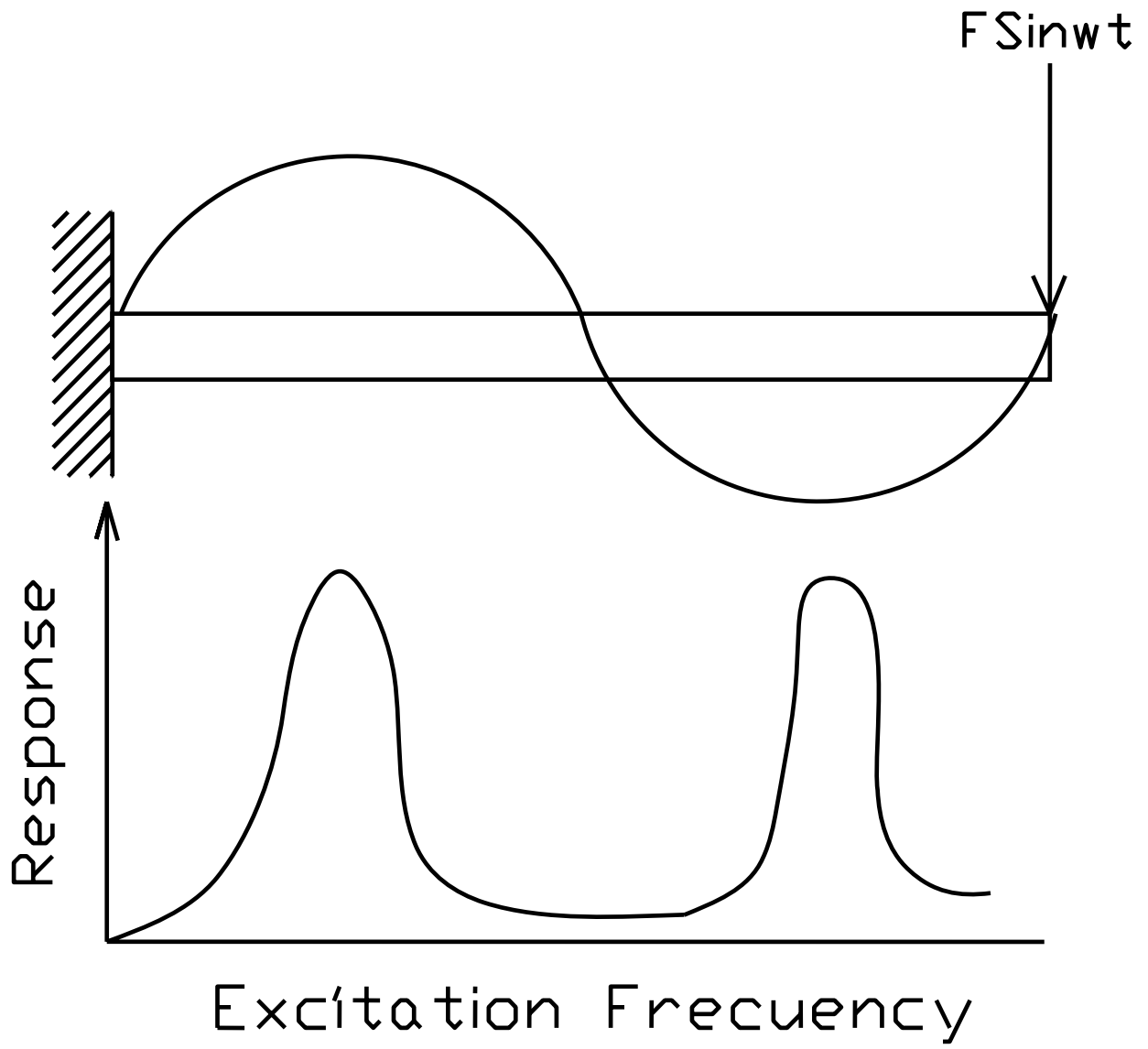


Fig 1.1

Parametric Resonance

In this case external excitation force is applied in the axial direction or perpendicular to the amplitude of vibration which leads to parametric resonance, when the excitation frequency or any integer multiple of it is twice the natural frequency. Here dynamic load component and excitation frequency is parametric with respect to the vibration.

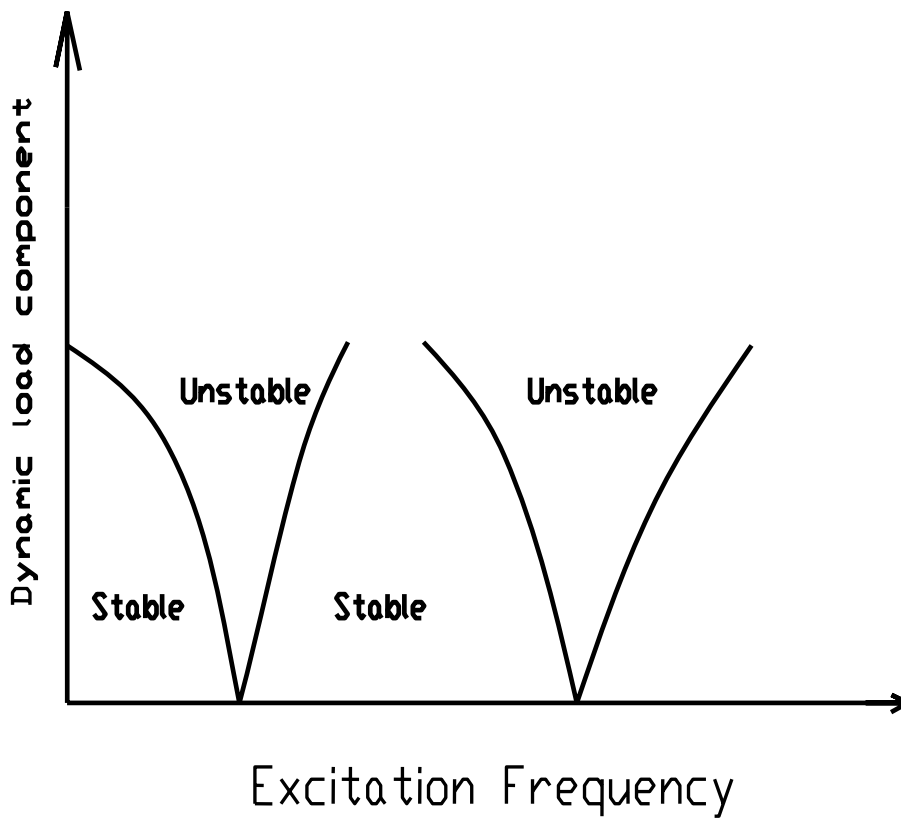
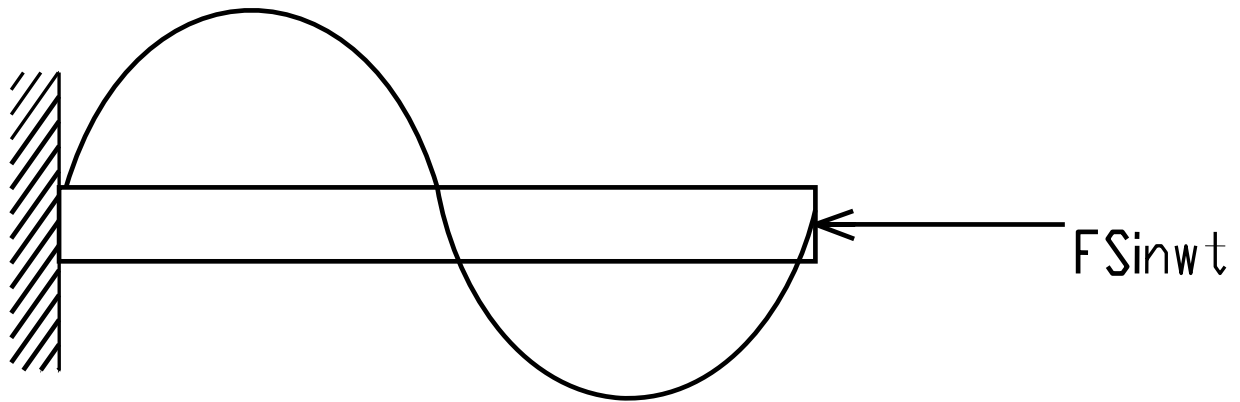


Fig 1.2

Condition of Parametric Instability

The system can experience parametric instability when the excitation frequency or any other integer multiple of it is twice the natural frequency that is to say

$$m\omega_e = 2\omega \quad ; \quad m= 1,2,3,\dots$$

The case of $\omega_e = 2\omega$ is known to be the most important in application and is called main parametric resonance. A vital step in the analysis of parametric systems is thus establishment of regions in the parameter space (plot between dynamic load component and excitation frequency) in which the system becomes stable, these regions are known as the regions of dynamic instability or zones of parametric resonance

The unstable regions are separated from stable ones by the so called stability boundaries and a plot of these boundaries on the parameter space is called STABILITY DIAGRAM.

Numerical method used for the analysis of dynamic stability systems

There are various numerical methods, out of which FINITE ELEMENT METHOD is used due to the following advantages,

- FEM is applicable to any field problem: heat transfer, stress analysis, magnetic field & so on.
- There are no geometric restrictions. The body region analyzed may have any shape.
- Boundary conditions and loading are not restricted.
- Material properties are not restricted to isotropy & may change from one element to another or even within an element.
- An FE structure closely resembles the actual body or region to be analyzed.
- The use of finite element for the simulation of rotor systems make it possible to formulate increasingly complicated problems, and also it has been established that more accurate results can be obtained only using for degrees of freedom.

Chapter 2

THEORETICAL ANALYSIS

THEORETICAL ANALYSIS

2.1 FINITE ELEMENT FORMULATION

A uniform cantilever shaft of length L , subjected to an axial compressive load $P(t)$ and rotating at a constant speed Ω is shown in the figure. A typical shaft element consists of two nodes and each node has four degrees of freedom: two translations and two rotations. With the axial motion neglected, a typical cross section of the shaft element, located at a distance s from the left node, in a deformed state is described by the translations $V(s, t)$ and $W(s, t)$ in the Y and Z directions and small rotations $B(s, t)$ about Y and Z . The translations (V, W) consist of a contribution (V_b, W_b) due to bending and as contribution (V_s, W_s) due to transverse shear deformation; the rotations (B, Γ) are only related to the bending deformations (V_b, W_b). The relationships can be expressed as follows

$$V(s, t) = V_b(s, t) + V_s(s, t); \quad W(s, t) = W_b(s, t) + W_s(s, t), \quad (1)$$

$$B(s, t) = -\partial W_b(s, t) / \partial s, \quad \Gamma(s, t) = \partial V_b(s, t) / \partial s \quad (2)$$

The translations and rotations of a typical point within the element can be related to the nodal displacement vector $[q^e]$ and the translational and rotational shape function $[N_t(s)]$ and $[N_r(s)]$ respectively as

$$\begin{Bmatrix} V(s, t) \\ W(s, t) \end{Bmatrix} = [N_t(s)] \{q^e(t)\}, \quad \begin{Bmatrix} B(s, t) \\ \Gamma(s, t) \end{Bmatrix} = [N_r(s)] \{q^e(t)\}, \quad (3,4)$$

where $\{q^e(t)\} = \{V_1, W_1, B_1, \Gamma_1, V_2, W_2, B_2, \Gamma_2\}^T$.

From equations (1)-(4), the two transverse shear strains $\{V_s', W_s'\}$ can be related to the nodal displacement vector as

$$\begin{Bmatrix} V_s' \\ W_s' \end{Bmatrix} = \left([N_t'] - \begin{bmatrix} 0 & 1 \\ -1 & 0 \end{bmatrix} [N_r] \right) \{q^e(t)\} = [B_s] \{q^e(t)\} \quad (5)$$

Where the symbol “ ’ ” indicates differentiation with respect to axial distance s . The representation of the shape function of the shape functions can be derived by using the expression of static deflection of a Timoshenko beam (Archer, 1965), and their detailed forms as well as the shape function matrices are as follows.

$$[N_t(s)] = \begin{bmatrix} \theta_1 & 0 & 0 & \theta_2 & \theta_3 & 0 & 0 & \theta_4 \\ 0 & \theta_1 & -\theta_2 & 0 & 0 & \theta_3 & -\theta_4 & 0 \end{bmatrix}$$

$$[N_r(s)] = \begin{bmatrix} 0 & -\phi_1 & \phi_2 & 0 & 0 & -\phi_3 & \phi_4 & 0 \\ \phi_1 & 0 & 0 & \phi_2 & \phi_3 & 0 & 0 & \phi_4 \end{bmatrix}$$

$$[B_s(s)] = \begin{bmatrix} \eta_1 & 0 & 0 & \eta_2 & \eta_3 & 0 & 0 & \eta_4 \\ 0 & -\eta_1 & \eta_2 & 0 & 0 & -\eta_3 & \eta_4 & 0 \end{bmatrix}$$

where

$$\theta_1 = [1 - 3\xi^2 + 2\xi^3 + (1 - \xi)\Phi] / (1 + \Phi),$$

$$\theta_2 = [1 - 2\xi^2 + \xi^3 + (\xi - \xi^2)\Phi/2] / (1 + \Phi),$$

$$\theta_3 = (3\xi^2 - 2\xi^3 + \xi\Phi) / (1 + \Phi),$$

$$\theta_4 = [1 - \xi^2 + \xi^3 - (\xi - \xi^2)\Phi/2] / (1 + \Phi),$$

$$\phi_1 = 6(-\xi + \xi^2) / [1(1+\Phi)],$$

$$\phi_2 = [1 - 4\xi + 3\xi^2 + (1-\xi)\Phi] / (1+\Phi),$$

$$\phi_3 = 6(\xi - \xi^2) / [1(1+\Phi)],$$

$$\phi_4 = (2\xi - 3\xi^2 + \xi\Phi) / (1+\Phi),$$

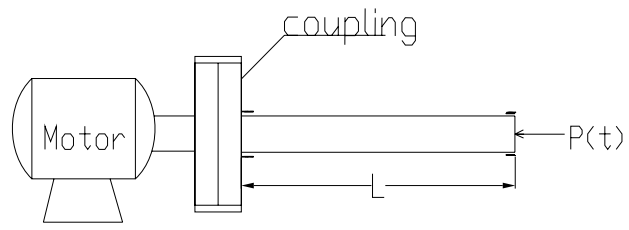
$$\eta_1 = \Phi / [1(1+\Phi)],$$

$$\eta_2 = \Phi / (1+\Phi),$$

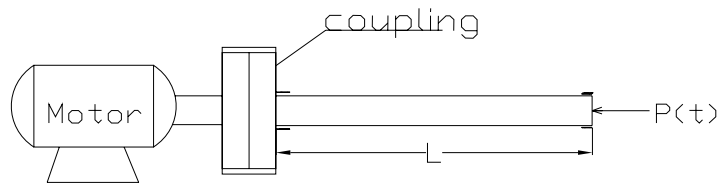
$$\eta_3 = \Phi [1(1+\Phi)],$$

$$\eta_4 = \Phi / (1+\Phi),$$

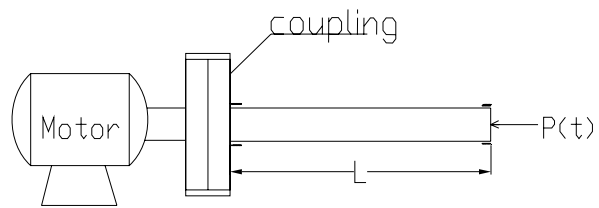
$$\xi = s/l, \quad \Phi = 12EI / (kGAL^2) \quad ,$$



Fixed--Fixed



Pinned-Fixed



Pinned--Pinned

2.2 FINITE SHAFT ELEMENT

The potential energy U^e of the uniform shaft element of length l , including the contributions of elastic bending and shear energy and the energy due to a spatial independent, axial compressive load P is given by

$$U^e = \frac{1}{2} \int_0^l EI [(V_b'')^2 + (W_b'')^2] ds + \frac{1}{2} \int_0^l kGA [(V_s')^2 + (W_s')^2] ds - \frac{1}{2} P \int_0^l [(V')^2 + (W')^2] ds \quad (6)$$

Where e is the Young's modulus, I is the second moment of area, k is the shear coefficient, G is the shear modulus and A is the cross-sectional area of the shaft.

Under the assumption that the shaft rotates at a constant speed Ω , the kinetic energy T^e of the shaft element including both the translational and rotational form is given by

$$T^e = \frac{1}{2} \int_0^l \rho A [(V')^2 + (W')^2] ds + \frac{1}{2} \int_0^l I_d [(B')^2 + (\Gamma')^2] ds - \frac{1}{2} \Omega \int_0^l I_p [\Gamma B - B \Gamma] ds + \frac{1}{2} \Omega^2 \int_0^l I_p ds$$

.....(7)

Where the symbol “ ‘ ” denotes the differentiation with respect to time t , ρ is the mass density of the shaft material, I_d and I_p are the diametrical and polar moments of inertia of shaft per unit length.

Upon substituting Equations (3)-(5) into equation (6)-(7), respectively the potential energy U^e and kinetic energy T^e can be rewritten in terms of the nodal displacement vector as,

$$U^e = \frac{1}{2} \{q^e\}^T [K_b^e] \{q^e\} + \frac{1}{2} \{q^e\}^T [K_s^e] \{q^e\} - \frac{1}{2} P \{q^e\}^T [K_g^e] \{q^e\}, \quad (8)$$

$$T^e = \frac{1}{2} \{q^e\}^T [M_t^e] \{q^e\} + \frac{1}{2} \{q^e\}^T [M_r^e] \{q^e\} - \frac{1}{2} \Omega \{q^e\}^T [H^e] \{q^e\} + \frac{1}{2} \Omega^2 I_p l \quad (9)$$

Where,

$$\begin{aligned} [K_b^e] &= \int_0^1 [N_r']^T EI [N_r'] ds; & [K_s^e] &= \int_0^1 [B_s]^T kGA [B_s] ds; \\ [K_g^e] &= \int_0^1 [N_t']^T [N_t'] ds; & [M_t^e] &= \int_0^1 [N_t]^T \rho A [N_t] ds \\ [M_r^e] &= \int_0^1 [N_r]^T I_d [N_r] ds; & [H_e] &= \int_0^1 I_p [N_r]^T \begin{bmatrix} 0 & 0 \\ 1 & 0 \end{bmatrix} [N_r] ds \end{aligned}$$

Upon substituting Equation (8) and (9) into Lagrange's equation, the equation of motion for the finite rotating shaft element is given as

$$\begin{aligned} ([M_t^e] + [M_r^e]) \{q^e\} - \Omega [G^e] \{q^e\} + ([K^e] - P [K_g^e]) \{q^e\} &= \{0\}, \\ [G^e] &= [H^e] - [H^e]^T \end{aligned} \quad (10)$$

2.3 SYSTEMS EQUATION OF MOTION:

The equation of motion of the complete system can be expressed as

$$[M]\{\ddot{q}\} - \Omega[G]\{\dot{q}\} + ([K] - P[S])\{q\} = \{0\}, \quad (11)$$

Where,

$$\begin{aligned} [M] &= \sum ([M_t^e] + [M_r^e]) \\ [G] &= \sum [G^e] \\ [K] &= \sum ([K_b^e] + [K_s^e]) \end{aligned}$$

For the case in which the shaft system is subjected to a periodic axial force of the form

$$P(t) = P_0 + P_1 \cos \theta t$$

Where θ is the axial disturbance frequency

The static and time dependent component of the load can be expressed as a fraction of the fundamental static buckling load P^* of the non-rotating Shaft as

$$P(t) = \alpha P^* + \beta P^* \cos \theta t \quad (12)$$

where α and β are referred to as the static and dynamic load factor respectively

If the two static and dynamic i.e. time dependent components of load are applied in the same manner, then equation (11) becomes

$$[M]\{\ddot{q}\} - \Omega[G]\{\dot{q}\} + ([K] - P^*(\alpha + \beta \cos \theta t)[S])\{q\} = \{0\} \quad (13)$$

Equation (13) represents a system of second order differential equation with periodic co-efficient of the Mathiew-Hill type. Application of the theory of linear equations with periodic

coefficients, the boundary between stable and unstable regions can be constructed by periodic solutions of period T and $2T$ (Bolotin 1964), where $T = 2\pi/\theta$. In dynamic stability problems, the usual interest is to determine the boundaries of principal instability region in frequency domain, in which the solution corresponds to the period of $2T$. As first approximation and putting attention only to the case of simple parametric resonance type, the parametric solution with period $2T$ can be sort in the form

$$\{q\} = \{a\}\sin(\theta t / 2) + \{b\}\cos(\theta t / 2) \quad (14)$$

By substituting Equation (14) into equation (13) and equating the coefficients of the $\sin(\theta t/2)$ and $\cos(\theta t/2)$ terms, a set of linear algebraic equations in terms of $\{a\}$ and $\{b\}$ is obtained as

$$([K] - P^*(\alpha - \beta/2)[S] - (\theta^2/4)[M])\{a\} + (\Omega\theta/2)[G]\{b\} = \{0\} \quad (15a)$$

$$([K] - P^*(\alpha - \beta/2)[S] - (\theta^2/4)[M])\{b\} + (\Omega\theta/2)[G]\{a\} = \{0\} \quad (15b)$$

The condition for the set of linear homogeneous equations, Equation (17) to have a nontrivial solution is

$$\begin{vmatrix} [K] - P^*(\alpha - \beta/2)[S] - (\theta^2/4)[M] & \Omega\theta/2[G] \\ -\Omega\theta/2[G] & [K] - P^*(\alpha + \beta/2)[S] - (\theta^2/4)[M] \end{vmatrix} = 0 \quad (16)$$

Equation (16) is referred to as the equation of boundary frequencies and can be used to construct the principal regions of dynamic stability.

Chapter 3

EXPERIMENTAL VALIDATION

EXPERIMENTAL VALIDATION

3.1 INTRODUCTION

The purpose of the present experimental work is to validate the theoretical results obtained from Finite Element Analysis and to find the instability and stability region for a rotating shaft system by plotting the stability diagram for it. For this purpose an experimental test rig was designed and fabricated.

3.2 DESCRIPTION OF EXPERIMENTAL SETUP

The main components of this set up are as follows:

1. Frame
2. DC Motor(1 HP)
3. Electrodynamic shaker(EDS)
4. Load cell
5. Vibration pick up
6. Oscillator and Power amplifier
7. Oscilloscope
8. Screw Jack

The test rig consists of a frame made up of steel channel section. The channel section of 6"×3" is used to provide sufficient strength and rigidity. The test rig is an inverted "U" shaped structure fixed to a concrete foundation with foundation bolts. Its approximate height is two meters and distance between the vertical columns is one meter.

A screw jack is fixed to the top horizontal bar of the frame. It is used to accommodate specimen of various length and also to apply static load on the specimen. A dc motor is rigidly attached to the screw jack, as shown in the figure. The specimen is attached to the motor by means of a sleeve coupling. A fluctuating load is applied to the other end of the specimen by means of the electrodynamic shaker (with frequency range of 0-3000 Hz and capacity 50 kgf). The dynamic load was measured by a load cell fitted to the moving table of shaker. The Electrodynamic Shaker is placed at the centre of the concrete foundation. The Electrodynamic Shaker is the key component of the set up. The EDS is connected to the power amplifier which is used to operate the EDS at desired frequency and amplitude. The pick up MM002 (Bruel & Kjaer,Denmark) is used to record the amplitude of external excitation frequency. It is placed at the top end of the specimen which is attached to the motor. The load cell is placed on the EDS table to record the Dynamic load acting on the specimen.

EXPERIMENTAL SETUP

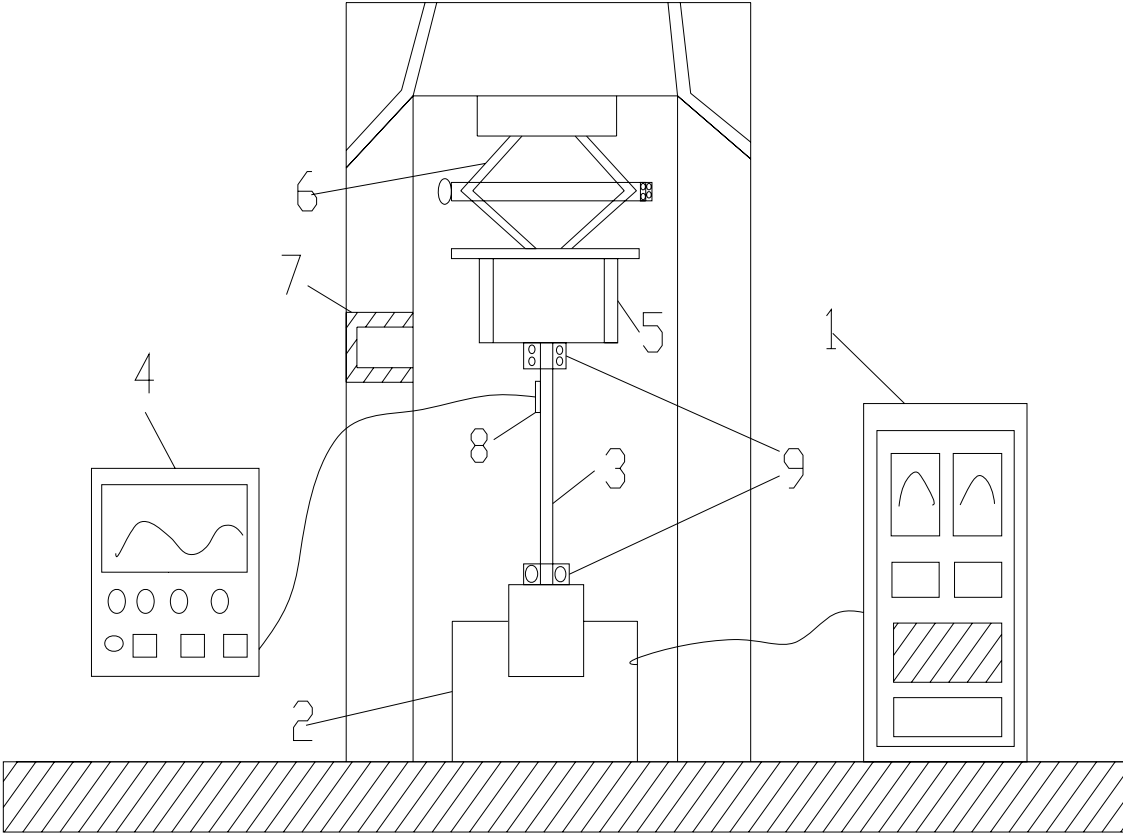


Fig-3.1

INDEX

- 1. Oscillator and power amplifier
- 2. Electro dynamic shaker
- 3. Specimen
- 4. Oscilloscope
- 5. D C Motor
- 6. Screw Jack
- 7. Frame
- 8. Accelerometer
- 9. End attachment

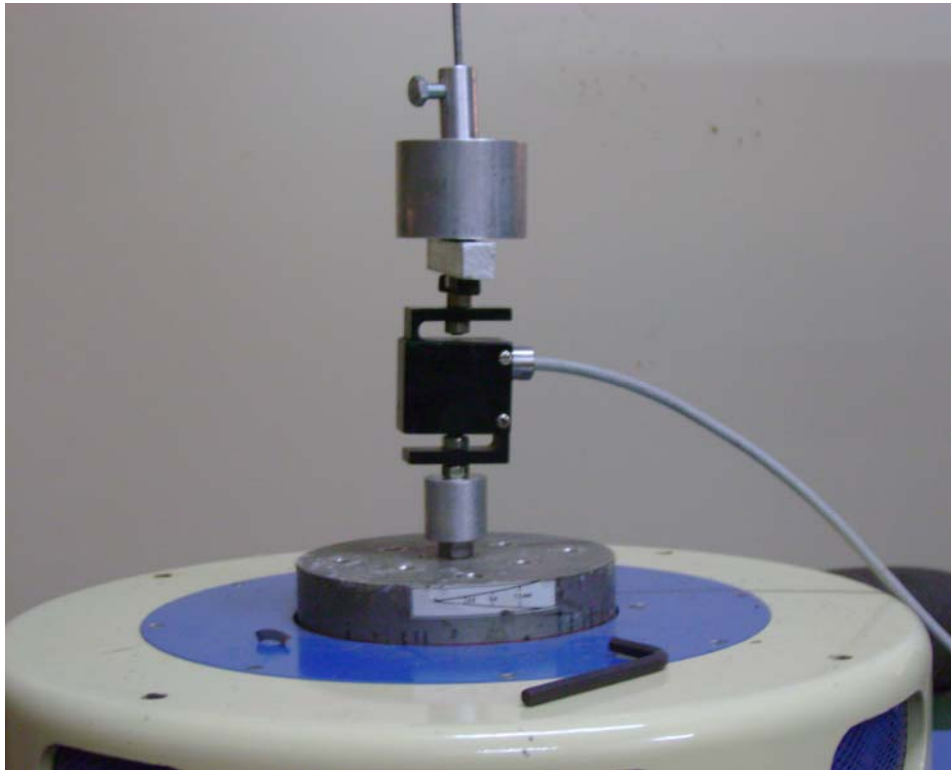


Fig-3.2 EXPERIMENTAL SET UP

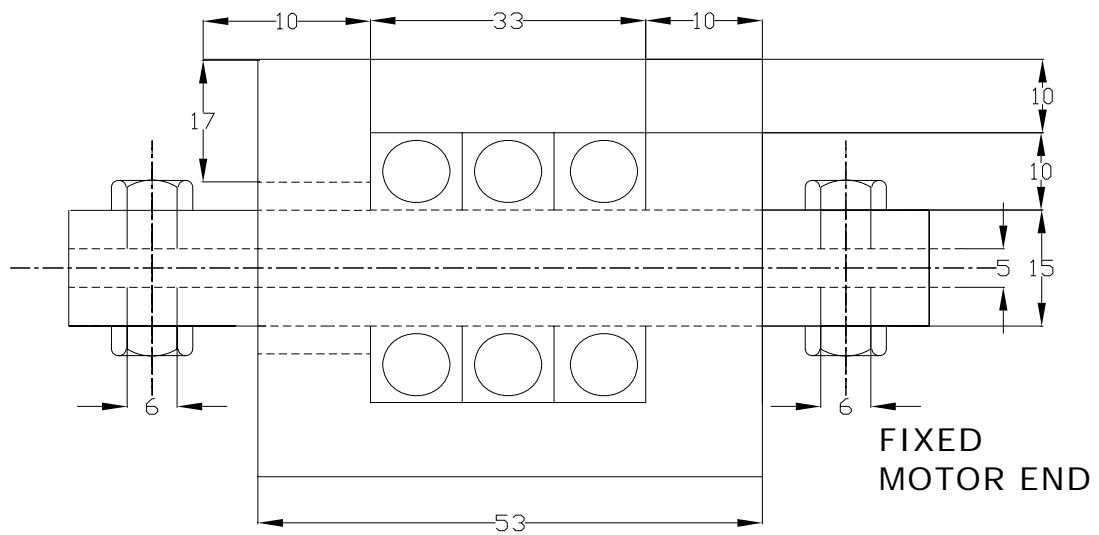


Fig-3.3

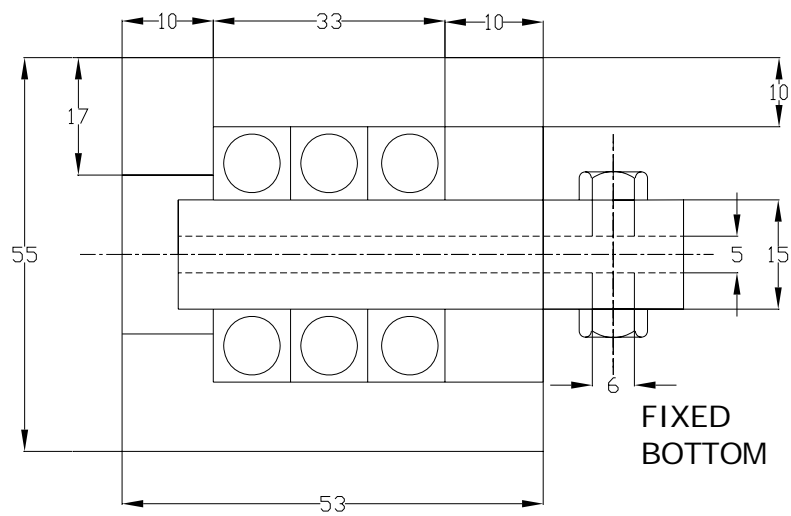


Fig 3.4

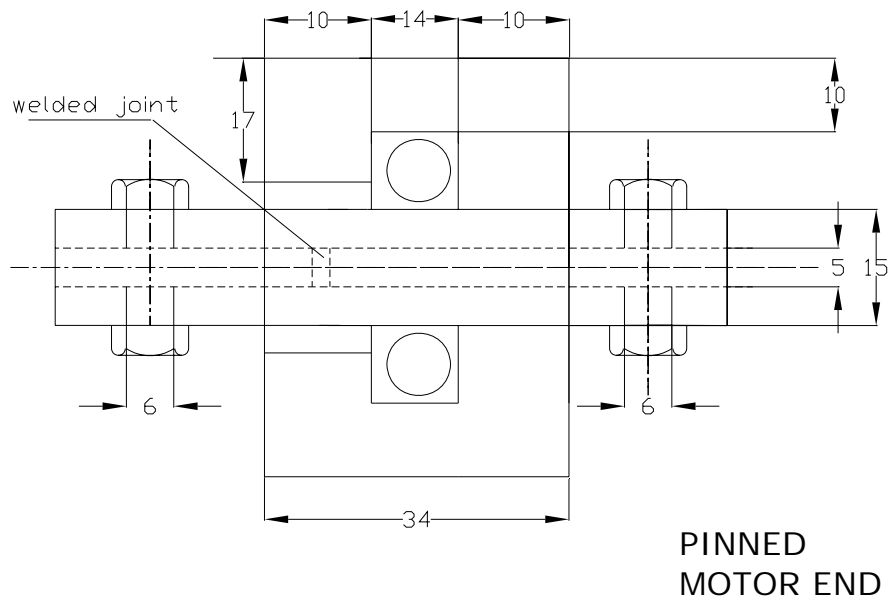


Fig 3.5

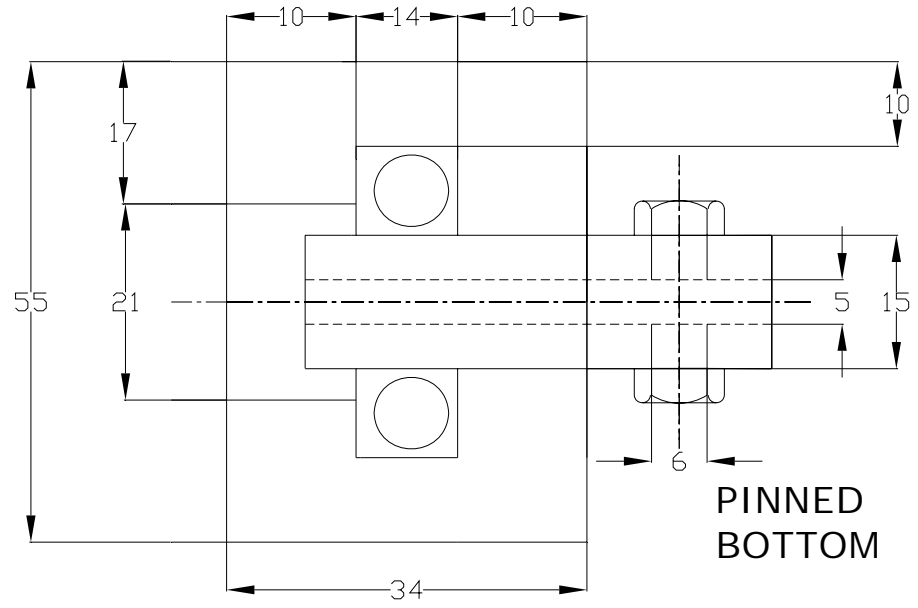


Fig 3.6

PICTURE OF END ATTACHMENTS



Fig 3.7

3.3 SPECIMEN PREPARATION

The specimen consists of a 4mm diameter GI wire. The length of the rod is 1.5m. The specimen is fitted to the end attachments in turn namely.,

Pinned motor ----- Pinned bottom.

Fixed motor ----- Pinned bottom.

Fixed motor ----- Fixed bottom.

3.4 EXPERIMENTAL PROCEDURE

The speed of the test specimen was controlled by the DC motor and its control circuit. The control circuit consists of two rheostats, one connected to the field and other connected to the armature. The speed of the motor is varied by changing the resistance of either the field or the armature. The specimen is run at constant speed. The rotational speed of the specimen which is equal to the speed of the motor was measured by tachometer. The dynamic load was applied to the specimen by means of Electro Dynamic Shaker. The displacement applied to the specimen at the bottom end is such that the vibration signal is visible at the oscilloscope. The displacement could be controlled by means of the amplifier or the shaker. Once the vibration signal was visible the amplitude was kept unchanged. Then the frequency of the dynamic load was increased by means of the oscillator of the power amplifier and oscillator unit of the shaker. The vibration signal of the test specimen was recorded by the vibration pickup. When the signal suddenly becomes very high the excitation frequency corresponds to the parametric resonance frequency which was noted down. The frequency of excitation was continuously increased and the frequencies at which the response becomes very high were noted down. These frequencies were divided by the first fundamental frequency (ω_0) of the system to give the frequency. The dynamic load factor β is calculated by dividing the dynamic load with the fundamental buckling load of the specimen. The unstable boundaries were established experimentally by plotting the points $\Omega/\omega_0, \beta$ and the theoretical and experimental results were compared.

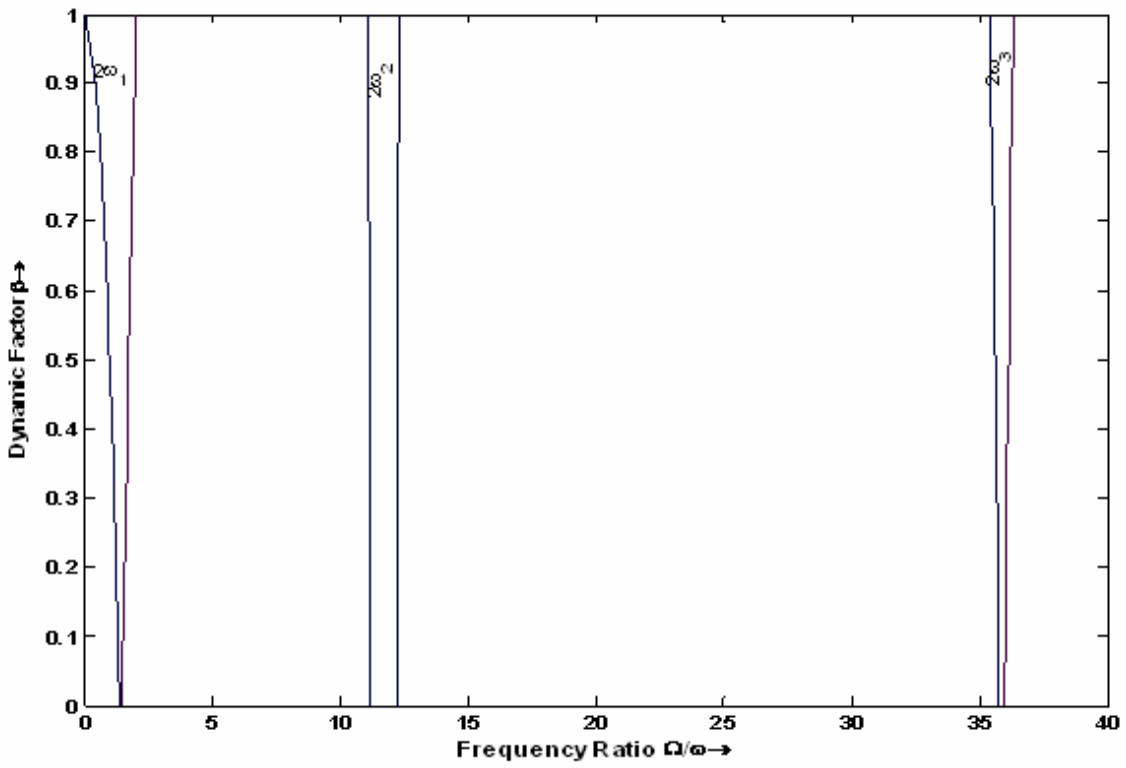
Chapter 4

RESULTS AND DISCUSSION

RESULTS AND DISCUSSION

The problem studied in this work is to determine the regions of Dynamic instability of a rotating shaft subjected to compressive load $P(t) = \alpha P^* + \beta P^* \cos \theta t$, where P^* is the static buckling load of the cantilever non-rotating shaft. The physical configurations for different end conditions are shown in figure 2.1, 2.2, 2.3 and the configuration and material properties are listed in table 4.1. A ten element discretisation gives good convergence of the first natural frequencies.

The rotational speed considered here is 2000 RPM stability regions for different end conditions are plotted in fig 4.1, 4.2, 4.3. Figure 4.1 is for fixed-pinned end condition, Figure 4.2 is for fixed-fixed end condition and figure 4.3 is for pinned-pinned end condition. It is observed that as the rotational speed increases, the boundary of region of dynamic instability are shifted outwardly, and width of the instability regions are increased, therefore the system becomes more unstable. Because gyroscopic moment is proportional to the rotational speed, it leads to the conclusion that the gyroscopic moment has destabilizing effect on the dynamic stability problem of the rotating shaft system. By comparing the nature of instability regions for the boundary conditions it is found that fixed fixed condition gives more stability to the rotating shaft system. Fig 4.4 shows the comparison of the theoretical and experimentally determined instability regions for $\Omega=2000$ RPM for Fixed-pinned condition. It shows matching between theory and experiment.



Instability Regions for Fixed Pinned End Condition, RPM2000

Fig-4.1

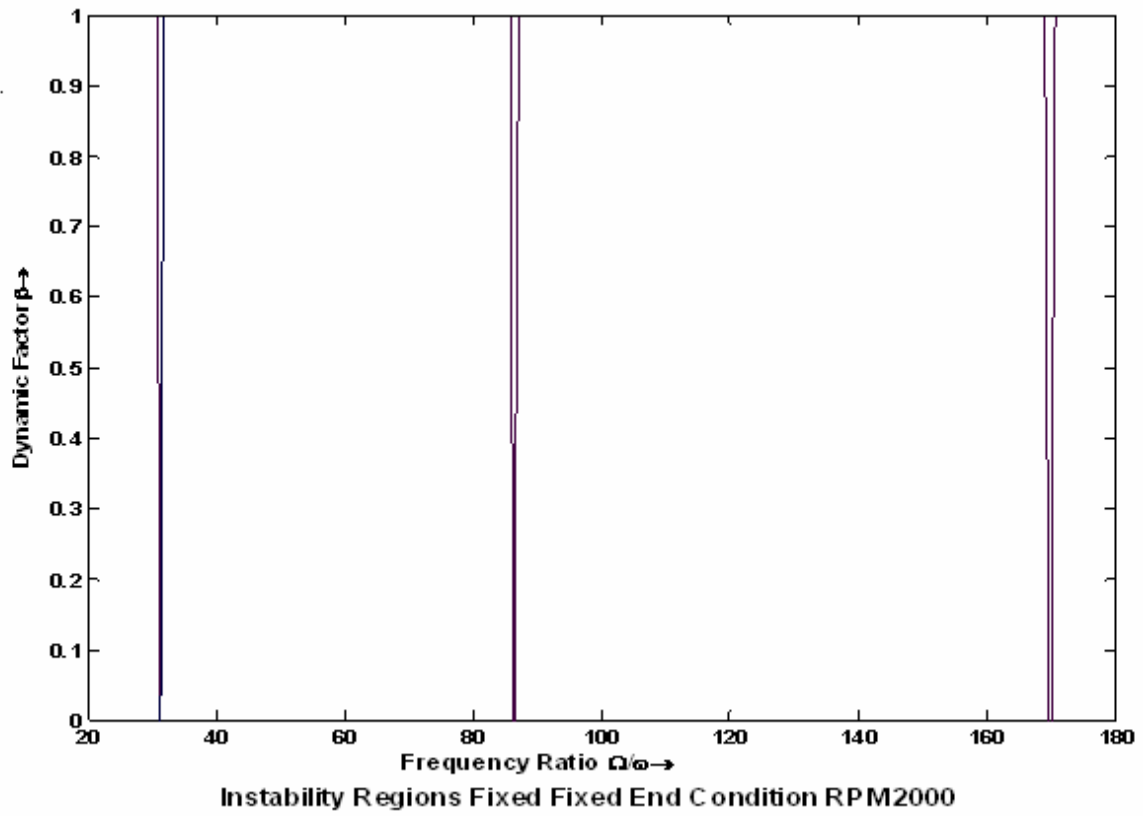


Fig-4.2

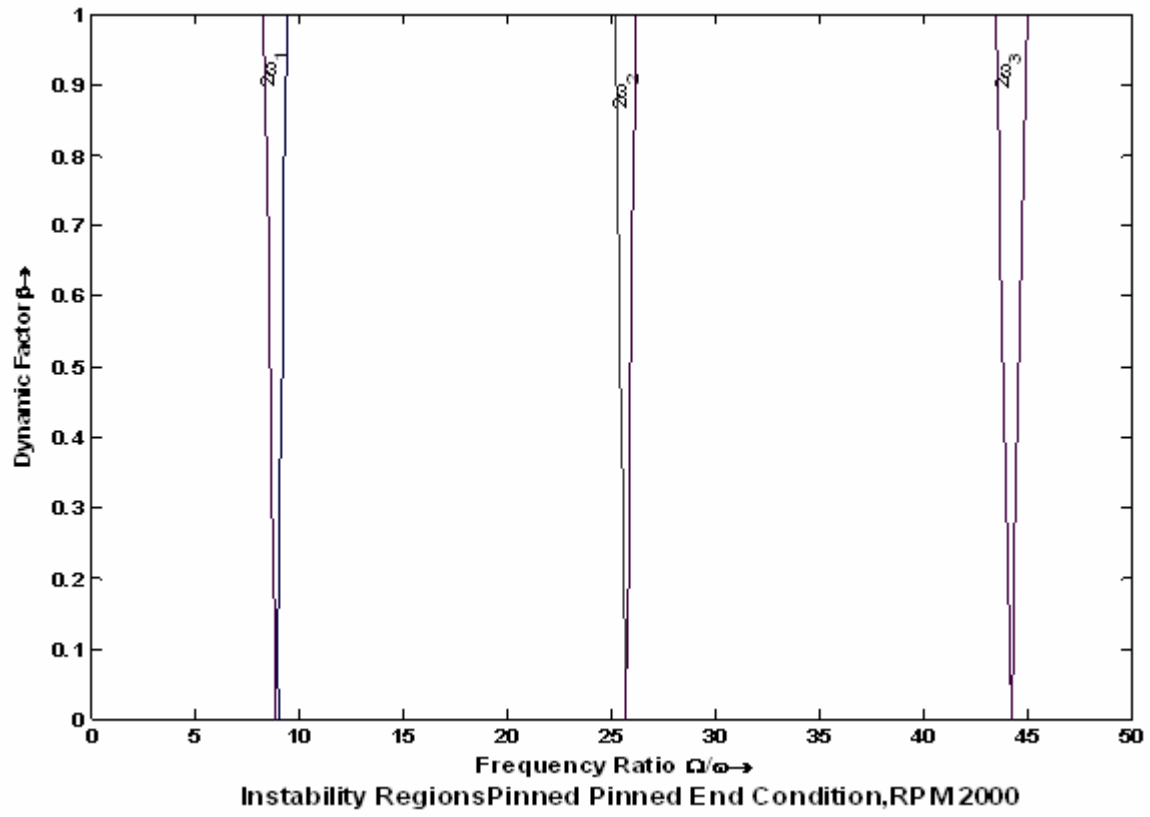


Fig 4.3

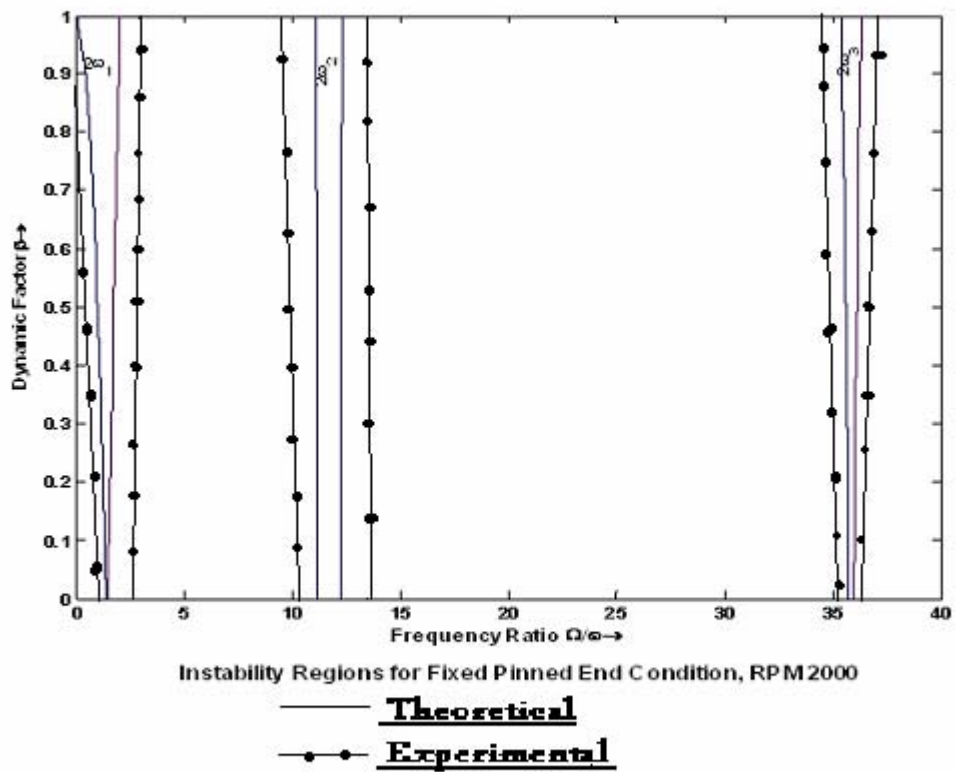


Fig 4.4

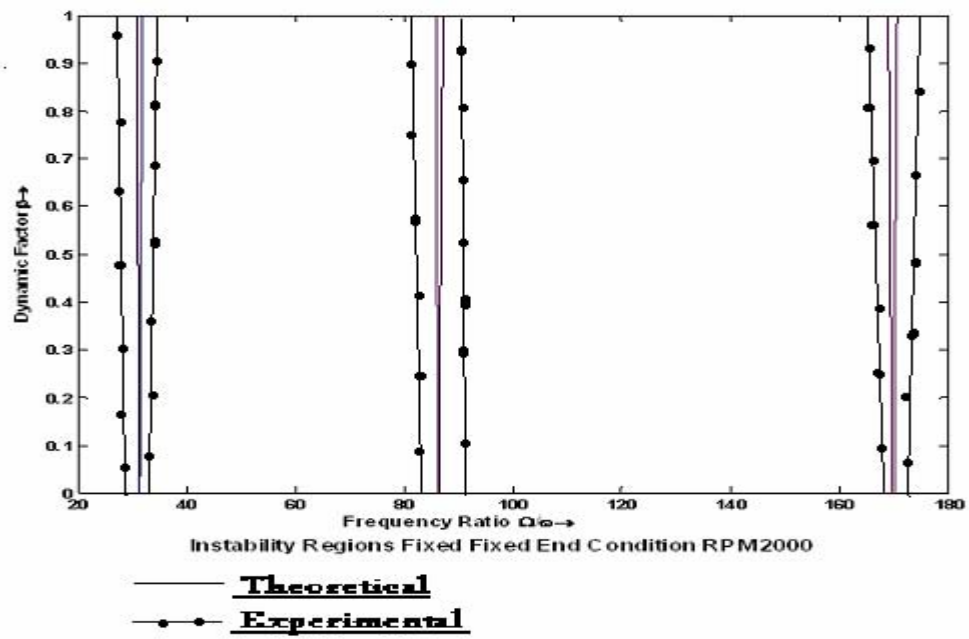


Fig 4.5

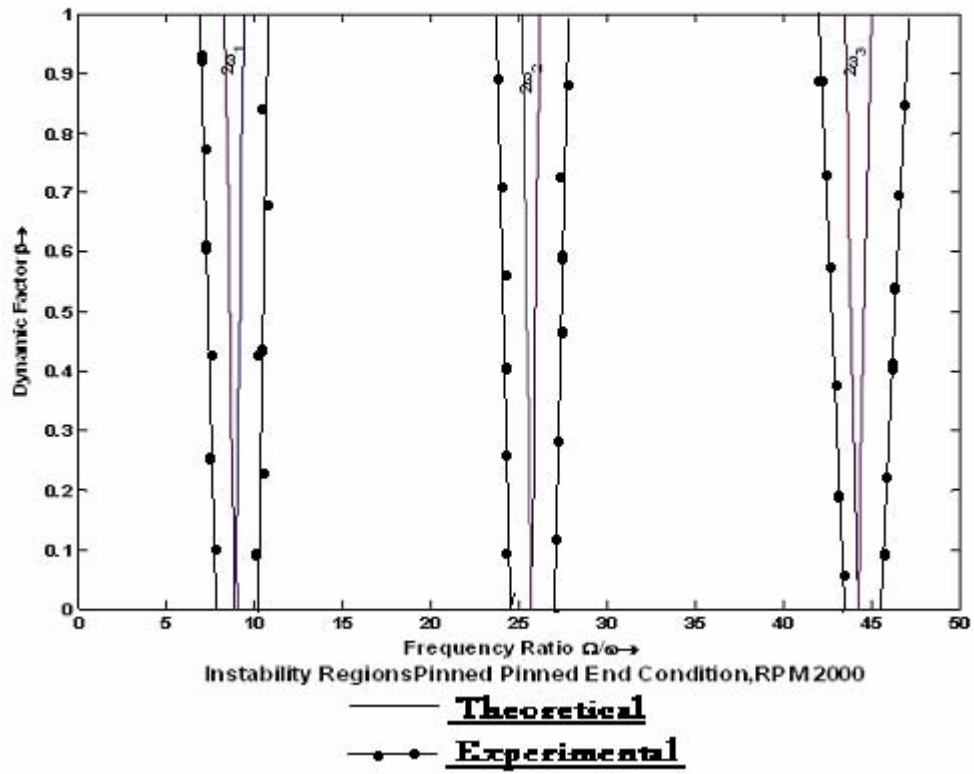


Fig 4.6

TABLE 4.1**CONFIGURATION DATA, MATERIAL PROPERTIES AND FORMULAE USED**

SL.NO.	QUANTITIES	VALUES
01	L	1.5m
02	D	4mm
03	m	0.27kg/m
04	P_{cr}	$\sqrt{EI/L^2}$
05	β	P_d/P_{cr}
06	$I=\pi/64 d^4$	$1.26*10^{-11}$
07	E	$2.1*10^{11}$ N/m ²
08	ρ	7500kg/m ³
09	ω	$\sqrt{EI/mL^4}$

Chapter 5

CONCLUSION

CONCLUSION

A Ritz finite element procedure employed to determine the regions of dynamic instability of a shaft subjected to periodic axial forces. By the use of Bolotin's method the equation of boundary frequencies can be obtained and instability regions were established by using Hsu's criteria. For the practical part, four end attachments were designed and fabricated.

The experiment was conducted for four different boundary conditions.

Numerical results show that the gyroscopic moment or the rotational speed can enlarge the regions of dynamic instability, and therefore the system becomes more unstable.

This type of parametric excitation is seen in shafts with long bearing, drill bits.

The graphs from theoretical analysis were plotted by simulation model and compared with the experimental graphs.

The experimental findings corroborate well with the theoretical results.

Chapter 6

REFERENCES

REFERENCES

1. Archer, J.S., 1965, "Consistent Matrix Formulations for structural analysis using Finite Element Techniques" AIAA Journal, Vol.3 pp 1910-1918.
2. Bolotin, V.V.,1964, " The Dynamic Stability of Elastic Systems", Holden Day. San-Francisco.
3. Loewy, R.G., and Piarulli, V.J., "Dynamics of Rotating Shafts", The shock and Vibration Centre, United States, Department of Defense.
4. Lund, J.W., and Orkutt, F.K., 1967, "Calculations and Experiments on the unbalance Response of a Flexible Rotor" ASME Journal of Engineering for Industry, Vol. 89, pp 785-796.
5. Mykelstad, N.O., 1944, "A New Method of Calculating Uncoupled Bending of Airplane wings and Other Type of Beams" Journal of Aeronautical Sciences. Vol.11, pp.153-162
6. Nelson, H.D., and Mc Vaugh, J.M., 1976, "The Dynamics of Rotor Bearing Systems Using Finite Elements" ASME Journal of Engineering for Industry, Vol.98 pp. 593-600.
7. Nelson, H.D., 1980, " A Finite Rotating Shaft Element Using Timoshenko Beam Theory," ASME journal of Mechanical Design, Vol.102,pp.793-803.
8. Ozguvamn, H.N.,and Ozkan, Z.L., 1984, " Whirl speeds and Unbalance Response of mlti Bearing Rotor Using Finite Elements", ASME journal of Vibration, Acoustics, Stress and Reliability in Design, Vol.106,pp.72-79.
9. Prohl, M.A., 1945, " A General Method of Calculating Critical Speed of Flexible Rotors", ASME journal of Applied mechanics, Vol,12 pp.142-148.

10. Rieger, N.F., 1977, "Rotor Bearing Dynamics- State of The Art", Mechanism and Machine Theory, Vol.12,pp.261-270.
11. Ruhl, R.L., 1970, "Dynamics of Distributed Parameter Turbo rotor System: Transfer Matrix and Finite Element Techniques." Ph.D. Thesis, Cornell University Ithaca,NY.
12. Ruhl, R.L. and Booker, J.F., 1972, "A Finite Element Model For Distributed Parameter Turbo-Rotor Systems," ASME Journal of Engineering for Industry, Vol.94,pp.128-132.